Modelling and Simulation of 2D-flow Suspension Diffusioosmosis

Sergio da Cunha, Nataliya Shcherbakova, Vincent Gerbaud, Patrice Bacchin[*]

Laboratoire de Génie Chimique, Université de Toulouse, CNRS, INP, UPS, Toulouse, France
patrice.bacchin@univ-tlse3.fr

Diffusioosmosis, also referred to as capillary osmosis, is the flow of a solution relative to a fixed object, where the flow is driven by solute concentration gradient. The solution considered here is an aqueous mixture containing colloids that flows in a channel and through an array of cylinders, representing a membrane. In this work we use an adaptation of the suspension balance model to investigate the influence of colloid – interface (Π_{ic}) interaction and colloid – colloid interactions (Π_{cc}) on the diffusioosmosis of a colloidal suspension. The model describes both osmosis and Marangoni flow, depending on the attractive or repulsive nature of Π_{ic}. Further, Π_{cc} dictates two important features of the flow. First, increasing the gradient of colloid concentration between the two channels by a factor of 10 increases the pressure drop by a factor of ~3.2 in the advection – osmosis equilibrium state. Second, including higher-order terms from the hard-sphere repulsion model (via the Carnahan-Starling equation of state) can increase colloid concentrations near the membrane by ~30%.

1. Introduction

The interaction between surfaces and pure fluid/mixtures has major applications in laboratory experiments as well as in the industry, like when chromatography or adsorption processes are operated. Two important interfacially-driven phenomena, nowadays known as diffusioosmosis and diffusiophoresis, were described by Derjaguin and co-authors in 1947 (Derjaguin et al., 1947). Authors noticed that particles may move spontaneously in a fluid mixture because of a concentration gradient of a different substance. This phenomenon upon which particle motion is driven by species gradient was called diffusiophoresis. Like diffusiophoresis, diffusioosmosis is also manifested under the presence of solute concentration gradients. Nevertheless, in the latter the solid surface is considered fixed, and the mixture flows around it.

In capillary osmosis, the concentration profile in the bulk can be set by connecting the openings of the capillary to reservoirs with different concentrations. The wall interacts with solute particles via attractive/repulsive forces along the y-direction perpendicular to the flow in the x-direction. These forces perpendicular to the wall are transmitted to the fluid, for example via viscous drag (Oster and Peskin, 1992). The resultant force on the solvent is usually written as the gradient of a term known as osmotic pressure. Osmotic pressure changes with respect to x, creating a hydrostatic pressure gradient along this direction due to momentum balance. Finally, this gradient is the driving force for the flow in the diffusive layer, which drives the fluid in the bulk (Anderson, 1989).

Diffusioosmosis is gaining attention in the micro/nanofluidics field. Fluid flow through confined system has many applications, including lab-on-a-chip analyses and microelectronics cooling (Laser and Santiago, 2014). Electroosmosis is commonly used to drive the flow, and it is preferred over diffusioosmosis because it is capable of generating larger flowrates. Nevertheless, solvophobic channel surfaces could induce hydrodynamic slip at the solid-fluid interface, which in turn amplifies significantly the diffusioosmotic flowrates in narrow channels (Ajdari and Bocquet, 2006). In addition, some biological processes may be attributed to diffusioosmosis. Bonthuis and Golestanian (2014) modeled the flow of a solution across a funnel-shaped membrane protein channel. Including diffusioosmotic effects and calculating the forces exerted on the channel's walls, they were able to predict the two conformational states (closed and opened) that the channel can adopt.

Diffusioosmosis is also one of the mechanisms driving the flow through membranes. Despite many models taking into account the membrane thickness (see for example Anderson and Malone (1974) and Marbach et al. (2017)), membranes are traditionally modeled as an infinitely thin boundary separating two homogeneous mixtures with different solute concentrations. The concentration difference generates a gradient in the so-called osmotic pressure, which drives solvent flow across the membrane. Bacchin (2017a) introduces an approach in which osmotic flow results from diffusioosmosis. The membrane-solute interaction was modeled as an energy barrier in a 1-D geometry.

We adapt Bacchin's (2017a) approach in a 2-D geometry to describe an aqueous mixture containing colloids that flows through an array of cylinders representing a membrane of finite thickness (see left sketch in Figure 1). Colloid – interface interactions are described as an attraction-repulsion potential (Π_{ic}), and colloid – colloid interactions (Π_{cc}) consist of two contributions: hard-sphere repulsion (Van't Hoff or Carnahan) and van der Waals (VDW) attraction. The first goal of this work is to determine whether this model predicts an increase in equilibrium pressure drop when colloid concentration difference across the membrane is increased. Further, we investigate the influence of Π_{ic} and Π_{cc} interactions on the diffusioosmosis of a colloidal suspension. Among other things, we intend to simulate moderate colloid adsorption near the membrane through modulation of Π_{ic}, and assess the drawback from using simplistic models in the description of colloid – colloid interactions.

2. Case study and balance equations

The case study in this work consists of a mixture of colloids and water flowing through an array of cylinders. Colloid concentration is fixed on the inlet and outlet, replicating a channel that connects two large reservoirs with certain colloid volume fractions (ϕ_l and ϕ_r). It is assumed that the cylinders are impermeable to both solute and solvent, and no-slip condition is imposed for the mixture at the cylinder's wall (Figure 1). The array of obstacles is simulated by using a single cylinder, together with symmetry conditions on the top and bottom boundaries of the domain. The coordinate system origin is set at the center of the cylinder. The blue rectangle in Figure 1 corresponds to the simulation domain, and its size can be arbitrarily chosen as long as L≫R.
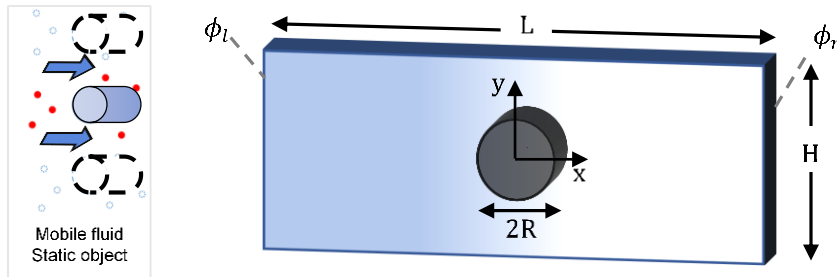

Figure 1: Sketch of the case study (left) and 2D geometry/domain used in simulations (right)

Domain size and boundary conditions are given in Table 1. In this table, u_l and u_r are the mixture's velocities at the left and right boundaries, respectively.

Table 1: Dimensions and boundary conditions used for the geometry show in in Figure 1

	R	L	H	ϕ_l	ϕ_r	$u_l{}^*$	$u_r{}^*$
SI	0.2 µm	4 µm	2 µm	0.01 − 0.1	0	0 µm/s	0 µm/s
Dimensionless	0.1	2	1	0.01 − 0.1	0	0	0

* To convert dimensionless velocities to SI units, multiply by 10.9 µm/s

An Euler-Euler approach is used to describe the suspension flow. In this approach, one does not keep track of individual particles. Instead, their properties (e.g. velocity) are assumed to be continuous. Because of this, the differential equations describing the particle phase are similar to those describing the fluid phase.

The equations used here, including repulsive – attractive colloid – interface interaction (Π_{ic}) and Van't Hoff's simple colloid – colloid (Π_{cc}) interaction models, are taken from the energy map model given in Bacchin (2017b) and Bacchin et al. (2019). We supplement it in this work with new colloid – colloid (Π_{cc}) interactions of repulsive and attractive nature. This model can be derived from the well-known Suspension Balance Model (Nott et al., 2011) at low colloid concentrations and neglecting inertia. Colloid – interface interactions are included as an attraction–repulsion potential (Π_{ic}), and colloid – colloid interactions (Π_{cc}) consist of two contributions: hard-

sphere repulsion and VDW attraction. Figure 2 sketches Π_{ic} for the purely repulsive and attraction + repulsion cases.
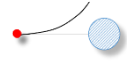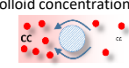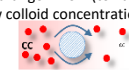

Figure 2: Colloid – interface interaction potential

Let $\boldsymbol{u}$ be the suspension's velocity, $\boldsymbol{J_\phi}$ be the colloid mass flux, and $\boldsymbol{\tau}$ be the viscous stress pressure, all in dimensionless form. The dimensionless steady state balance equations for the suspension flow are given by:

$$\nabla . \boldsymbol{u} = 0 \tag{1}$$

$$\nabla . \boldsymbol{J_\phi} = 0 \tag{2}$$

$$\nabla . (\boldsymbol{\Pi_m} + \boldsymbol{\tau}) = \boldsymbol{0} \tag{3}$$

If μ is the suspension's viscosity, ϕ is colloid volume fraction and K is mobility, the equations describing the irreversible processes in the system are:

$$\boldsymbol{\tau} = -\mu(\phi)(\nabla \boldsymbol{u} + \nabla \boldsymbol{u}^T) \tag{4}$$

$$\boldsymbol{J_\phi} = \phi \boldsymbol{u} - K(\phi)(\nabla \Pi_{cc} + \phi \nabla \Pi_{ic}) \tag{5}$$

The equations of state for $\nabla . \boldsymbol{\Pi_m}$, Π_{ic} and Π_{cc} are:

$$\nabla . \boldsymbol{\Pi_m} = \nabla[(1 - \phi)p] + \phi \nabla \Pi_{ic} \tag{6}$$

$$\Pi_{ic} = (1 + a_{tt})ke^{-\frac{d}{l}} - a_{tt}ke^{-\frac{d}{2l}} \tag{7}$$

$$\Pi_{cc} = \text{hard sphere repulsion + vdw attraction} \tag{8}$$

where p is the hydrostatic pressure, d is the distance to the cylinder's surface, and a_{tt}, k, l are a set of parameters used to describe interface-colloid interactions. The contributions to Π_{cc} in Eq(8) are:

$$(\text{repulsion}) \ \Pi_{van't\,Hoff}(\phi) = \phi$$

or
$$\tag{9}$$

$$(\text{repulsion}) \ \Pi_{Carnahan}(\phi) = \phi \frac{1 + \phi + \phi^2 - \phi^3}{(1 - \phi)^3}$$

$$(\text{attraction}) \ \Pi_{vdw}(\phi) = -\frac{z_n A}{36 k_B T} \frac{\phi^3}{\left(\phi_{cp} - \phi_{cp}^{1/3} \phi^{2/3}\right)^2} \tag{10}$$

The model enables description of osmosis and Marangoni-like flow, depending on the occurrence of colloid – interface attraction (Bacchin et al., 2019). Purely repulsive colloid – interface interactions (i.e., $a_{tt} = 0$ in Eq(7)) create a spontaneous fluid flow towards the higher colloid concentration zone (osmosis), even when hydrostatic pressure difference is 0. When long-range interface – colloid attraction is included, the fluid can flow in the opposite direction, i.e. towards lower colloid concentrations (Marangoni-like flow). Here however, we do not focus on the spontaneous flow generated without pressure difference. Instead, the results shown in the next section depict the advection–osmosis equilibrium, when pressure difference prevents flow between the reservoirs. More specifically, this study portrays the impact of colloid concentration, attraction parameter and colloid-colloid interaction on this equilibrium state.

Note that an absence of flow between the reservoirs does not mean that the mixture is stagnant in the channel. Indeed, as Figure 3 shows, the mixture circulates inside it without crossing the left/right boundaries. Simulations were run using FiPy – a python-based partial differential equation solver (Guyer et al., 2009). The SIMPLE

algorithm (Patankar and Spalding, 1972) was implemented to solve the Navier-Stokes equations in a collocated grid, using the Rhie-Chow interpolation to estimate the velocity at the cells' edges (Pascau, 2011).

3. Results

Mixture's velocity and concentration profiles corresponding to advection–osmosis equilibrium are displayed in rows in Figure 3. Two different colloid concentration values were imposed at the left boundary: $\phi_l = 0.01$ in the first line and $\phi_l = 0.1$ in the subsequent lines. At the right boundary, ϕ_r was kept at 0 in all simulations. Comparing the first and second lines in Figure 3, we observe that an increase in colloid concentration difference between the reservoirs increases the mixture's velocity. This is expected since the body force on the mixture ($\phi\underline{\nabla}\Pi_{ic}$, see Eq(6)) is proportional to the colloid concentration. Interestingly, the profiles' appearance does not change significantly upon an increase in colloid concentration. But a shift in the absolute values of velocities and concentration is observed. Finally, the pressure drop along the x-axis for the case $\phi_l = 0.01$ (first line) is of +0.00128 (multiply by 982 Pa to obtain pressure in SI units). The positive value indicates that the left boundary has a higher pressure than the right one. This pressure difference is what equilibrates the osmotic tendency for the mixture to flow towards higher solute concentrations. When concentration at the left boundary is increased (line 2), this tendency is enhanced and a higher pressure drop (+0.00414) is required to attain the advection–osmosis equilibrium.

When long-range attraction is included (line 3), colloids concentrate around the cylinder, forming the red ring. The velocity profiles are more complex in this case, with the appearance of extra vortices. Furthermore, the flow seems to have been partially inverted after increasing the attraction parameter a_{tt} (line 3 vs line 2). Blue areas in the velocity profiles on the second row become red on the third row, and vice-versa. The pressure drop corresponding to the third line of results is -0.0147. It is negative because the flow tends to move towards low colloid concentrations (from left to right) when $a_{tt} = 0.2$, so a higher pressure at the right boundary is necessary to attain equilibrium.

Note that the equation of state (EoS) changes between the second and third lines. On the second line in Figure 3, the van't Hoff equation is used to model hard-sphere repulsion. The next line adds the VDW contribution to account for attraction between colloid particles. Nevertheless, this addition has very little effect on the particle pressure Π_{cc}. At $\phi = 0.1$, its value changes from 0.100 (van't Hoff) to 0.097 (van't Hoff + VDW). Therefore, we can assume that the changes in concentration and velocity profiles between lines 2 and 3 in Figure 3 are exclusively due to the increase in the attraction parameter.

Finally, the last line displays results when using the Carnahan-Starling + VDW EoS. It shows that the profiles change significantly according to how the colloids interact with each other. When the van't Hoff EoS is used to describe the colligative properties of colloids (lines 1 and 2), one neglects the impact of colloid – colloid interactions on the effective diffusion coefficient. Indeed, van't Hoff law implies $\underline{\nabla}\Pi_{cc} = \underline{\nabla}\phi$ in Eq(5), and only hydrodynamic interactions, captured by $K(\phi)$, affect the effective diffusivity of colloids. The inclusion of the VDW term (line 3) does not have a significant impact on the model, and $\underline{\nabla}\Pi_{cc} \approx \underline{\nabla}\phi$. When Carnahan-Starling + VDW EoS are used (line 4), we describe colloid interactions with a more complex repulsive term. In this case $\underline{\nabla}\Pi_{cc} = (d\Pi_{cc}/d\phi)\underline{\nabla}\phi$. The effect of the colloid – colloid interactions on the diffusivity is now captured by the derivative of the particle pressure with respect to ϕ.

In particular, the diffusivity close to the left boundary of the domain ($\phi = 0.1$) is higher than the diffusivity at the right boundary ($\phi = 0$). This difference generates some colloid accumulation in the domain. Indeed, we observe that the average colloid concentration ϕ in the channel increases from 0.0576 (line 3) to 0.0638 (line 4). As a result, the colloid ring formed around the cylinder becomes much more pronounced. Colloid concentration peaks at ~0.16 in that area, which corresponds to a 60 % increase with respect to the concentration at the left boundary. At higher volume fractions, that could result in the formation of cakes around the cylinder.

The velocity profiles reflect this change in colloid distribution. When Carnahan + VDW EoS are used to model the particle interactions, the colloid distribution around the cylinder is nearly symmetric. In other words, colloid concentration can be approximated as a function of the distance to the cylinder ($\phi \approx \phi(d)$) in the region $d < 3.5R$, with R being the cylinder's radius. Furthermore, Eq(7) shows that Π_{ic} depends only on the distance d. Therefore, the body force term $\phi\underline{\nabla}\Pi_{ic}$ in Eq(6) is almost radial close to the cylinder. This means that it can be approximated as a gradient of some function in the range $d < 3.5R$. Hence, this force can be balanced by the pressure profile, in the same way that pressure balances the gravitational force in a water bottle. This explains why the absolute velocity values decrease from the third to the fourth lines. Pressure drop changes as well, from -0.0147 with van't Hoff + VDW EoS to -0.0121 using Carnahan + VDW EoS.
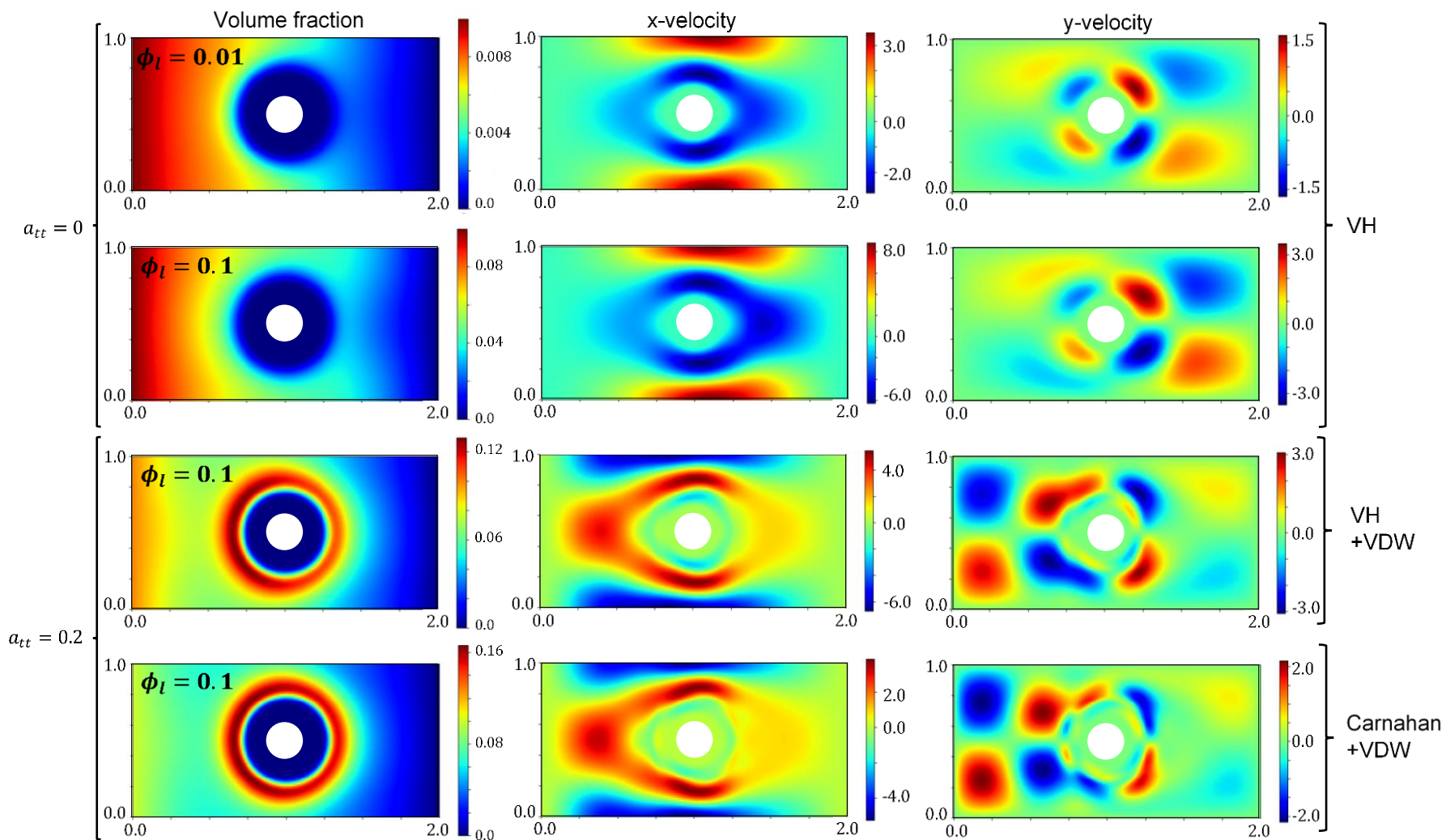
Figure 3: Colloid and velocity profiles at advection–osmosis equilibrium. Simulations are performed for different colloid-cylinder interactions (with the parameter a_{tt}) and for different EoS for colloids, which include a van't Hoff (VH) or Carnahan repulsion term and a Van der Waals (VDW) attraction term.

4. Conclusion

In this work, we have studied the advection–osmosis equilibrium in a system representing a membrane in a channel connecting two reservoirs with different colloid concentrations. Membrane's selectivity is modeled via the energy map Π_{ic} in Eq(7) that describes interface – colloid interactions. Numerical results show that higher colloid concentration differences require higher pressure drop to prevent the mixture from flowing between the reservoirs (advection–osmosis equilibrium). This agrees qualitatively with classic results for membranes. Further, the higher concentration differences increase velocity in the channel.

The inclusion of long-range attraction (by setting $a_{tt} = 0.2$ in Eq(7)) creates an adsorption zone around the cylinder. This result, also reported in Bacchin et al. (2019), suggests that long-range interface – colloid attraction could accelerate cake formation by increasing solute concentration near the membrane. Overall, the flow becomes more complex, with several vortices forming in the domain, and the pressure drop can be inverted if the attraction is sufficiently strong.

Finally, we have investigated the influence of colloid – colloid interaction Π_{cc} on a system with long-range colloid-interface attraction. The main result from this investigation is that the van't Hoff model underestimates the increase in colloid concentration around the cylinder. This is because colloid diffusivity in such model does not depend on absolute colloid concentration, whereas in reality this diffusivity increases with respect to colloid concentration in the low ϕ range ($\phi < 0.35$ considering Carnahan + VDW EoS). Because of this dependency, the boundary richer in colloid has higher colloid diffusivity, resulting in an average colloid concentration higher than the one predicted with the Van't Hoff model. This larger average concentration is the reason for the higher concentration peak ($\phi_{max} \sim 0.16$) in the last row of Figure 3. For larger concentration differences and/or stronger attraction interactions, van't Hoff model will underestimate the potential for cake formation due to these concentration peaks.

References

Ajdari A., Bocquet L., 2006, Giant amplification of interfacially driven transport by hydrodynamic slip: Diffusio-osmosis and beyond, Phys. Rev. Lett., 96, 1–4.

Anderson J., Malone D.M., 1974, Mechanism of Osmotic Flow in Porous Membranes, Biophysical Journal, 14, 957–982.

Anderson J., 1989, Colloid Transport By Interfacial Forces, Annu. Rev. Fluid Mech., 21, 61–99.

Bacchin P., 2017a, Colloid-interface interactions initiate osmotic flow dynamics, Colloids and Surfaces A, 533, 147–158.

Bacchin P., 2017b, An energy map model for colloid transport, Chem. Eng. Sci., 158, 208–215.

Bacchin P., Glavatskiy K., Gerbaud V., 2019, Interfacially driven transport theory: A way to unify Marangoni and osmotic flows, Phys. Chem. Chem. Phys., 21, 10114–10124.

Bonthuis D.J., Golestanian R., 2014, Mechanosensitive Channel Activation by Diffusio-Osmotic Force, Phys. Rev. Lett., 113, 148101.

Derjaguin B. V., Sidorenkov G.P., Zubashchenkov E.A., Kiseleva E.V., 1947, Kinetic Phenomena in Boundary Films of Liquids, Kolloidn. Zh., 9, 335–347.

Guyer J.E., Wheeler D., Warren J.A., 2009, FiPy: Partial Differential Equations with Python, Computing in Science & Engineering, 11, 6–15.

Laser D.J., Santiago J.G., 2004, A review of micropumps, J. Micromech. Microeng., 14, R35–R64.

Marbach S., Yoshida H., Bocquet L., 2017, Osmotic and diffusio-osmotic flow generation at high solute concentration. I. Mechanical approaches, J. Chem. Phys., 146, 194701.

Nott P.R., Guazzelli E., Pouliquen O., 2011, The suspension balance model revisited, Phys. Fluids, 23, 043304.

Oster G., Peskin C.S., 1992, Dynamics of osmotic fluid flow, Chapter In: T.K. Karalis (Ed.), Mechanics of Swelling. Springer, Berlin, 731–742.

Pascau A., 2011, Cell face velocity alternatives in a structured colocated grid for the unsteady Navier–Stokes equations, Int. J. Numer. Meth. Fluids, 65, 812–833.

Patankar S.V., Spalding D.B., 1972, A Calculation Procedure for Heat, Mass and Momentum Transfer in Three-Dimensional Parabolic Flows, Int. J. Heat Mass Transfer, 15, 1787–1806.